

# THE APPLICATION OF FINITE-ELEMENT ANALYSIS IN THE DESIGN OF THICK-FILM HYBRID CIRCUITS

Marina Santo Zarnik

HIPOT - R&D, Šentjernej, Slovenia

**Key words:** electronics, electronic components, electronic circuits, hybrid circuits, thick film circuits, circuit design, circuit analysis, FEM, Finite-Element Method, FEA, Finite-Element method Analysis, temperature distribution, power circuits, laser cuts, electrical properties, thermal properties, numerical simulations, optimization

**Abstract:** In this paper, practical examples of the application of finite-element analysis (FEA) in the design of hybrid thick-film circuits are presented. The electro-thermal behaviour of the circuits was modelled. Simulations were used to predict the resistance and steady-state temperature distribution of differently shaped thick-film resistive elements. A simulation-based analysis of resistor geometry and its position enabled the designer to optimise the circuit layout. In another example, FEA provided a means for visualising the transient-temperature field distribution in a hybrid thick-film circuit. Simulations were used to determine the optimum resistor dimensions and position. The presented examples show how simulations at an early stage of the design phase, or later in the redesign phase, can help to find the required solutions.

## Uporaba analize po metodi končnih elementov pri načrtovanju debeloplastnih hibridnih vezij

**Ključne besede:** elektronika, deli sestavni elektronski, vezja elektronska, vezja hibridna, vezja debeloplastna, snovanje vezij, analiza vezij, FEM metoda elementov končnih, FEA analiza po metodi elementov končnih, porazdelitev temperature, vezja močnostna, rezi laserski, lastnosti električne, lastnosti termične, simulacije numerične, optimiranje

**Izvleček:** V prispevku so opisani primeri uporabe analize po metodi končnih elementov pri načrtovanju hibridnih debeloplastnih vezij. Poseben poudarek je na modeliranju in simulaciji elektro-termičnih lastnosti debeloplastne strukture. Prikazane so simulacije debeloplastnega upora, ki so omogočile izračun upornosti poljubno oblikovanih uporov in analizo vpliva laserskega reza na njihove električne in termične lastnosti. Analiza segrevanja debeloplastnega upora v odvisnosti od njegovih dimenzij, oblike in pozicije na močnostnem debeloplastnem vezju je omogočila optimizacijo dizajna vezja. Simulacije prehodnih termičnih razmer so omogočile vpogled v temperaturno porazdelitev pri kratkotrajnih močnostnih obremenitvah in nakazale možnosti za izboljšanje dizajna hibridnega debeloplastnega linijskega zaščitnega modula. Obravnavani primeri kažejo kako lahko numerične simulacije pomagajo načrtovalcu poiskati optimalno rešitev.

### 1. Introduction

Thanks to the exponential increase in computational power in recent years and the continuous refinement of design-analysis tools, the numerical modelling and simulation of physical entities has become a more and more commonly used technique in electronic system design. Such an approach gives us the opportunity to study a circuit design prior to committing to layout and building the real prototypes. Designers are increasingly relying on simulations, especially in the design of micro-electro-mechanical systems (MEMSs), which results in a need for multi-physics, e.g. structural, electrical and thermal coupled-field analysis. The advantage of the virtual prototyping can be used in the design of the hybrid thick-film circuits, too. The simulations of the heat-transfer mechanisms, which allow the designer to predict the temperature distribution and the flow field in and around the circuit, are helpful in designing reliable devices [1-7].

Consideration of the thermal phenomena is especially important in the design of power hybrids. Under real operating conditions the hybrid thick-film circuit as well as the individual (active or passive) electronic components belonging to it are subjected to a variety of loading condi-

tions that either directly or indirectly influence their operating temperatures. The inappropriate placement of components may cause undesirable peaks in the temperature distribution that can influence the circuit's performance, reduce its reliability and shorten its lifetime. Simulations can help to reveal the critical points in the design and find the best design solution.

In this paper we first sketch out the basic principles of modelling electro-thermal properties.

Next, examples showing how simulations in the design phase of hybrid thick-film circuits have helped to achieve good thermal management of the product are presented.

Finally, we provide a summary and draw conclusions.

### 2. Modelling electro-thermal properties

A mathematical model of a certain physical situation is a system of differential equations that are derived by applying the fundamental laws and principles of nature to the treated system with a set of corresponding boundary and initial conditions.

## 2.1 Electrical conduction in thick-film resistors

When a voltage is applied across different parts of an electrically conducting object (e.g. a thick-film resistor) an electric current field is created within its volume. The electric current density  $J$  is simply related to the field strength  $E$  by the relation:

$$J = \gamma \cdot E = -\gamma \cdot \nabla U \quad (1)$$

where  $\gamma$  is electrical conductivity. Conservation of charge requires that:

$$\nabla \cdot J + \frac{\partial q}{\partial t} = 0 \quad (2)$$

where  $q$  is the charge density. This equation simply means that the current diverging from a volume element is equal to the rate of decrease of its charge. If we deal with static phenomena the time derivative is zero and by combining equations (1) and (2) we obtain:

$$\nabla \cdot (-\gamma \nabla U) = 0 \quad (3)$$

Having calculated the potential distribution we obtain the current density everywhere inside the treated structure by taking the gradient. As shown below, these equations can be used for the calculation of the resistance of an arbitrarily shaped thick-film resistor and to analyse different shapes of laser trim cuts.

## 2.1 Modelling heat-transfer mechanisms

In general, there are three heat-transfer mechanisms that describe the heat-flow field in and around a given solid structure: conduction, convection and radiation.

The phenomenon of thermal conduction involves the transfer of energy in the form of heat in a non-uniformly heated solid body. The differential equation governing the heat conduction in a homogenous body is:

$$\nabla(-\lambda \cdot \nabla T) + \frac{\partial T}{\partial t} \cdot \rho \cdot c_p - q_v = 0 \quad (4)$$

where  $\lambda$  is the thermal conductivity,  $T$  is the temperature,  $\rho$  is the material density,  $c_p$  is the specific heat, and  $q_v$  is the amount of heat evolved by internal sources in the body per unit volume.

In a wide range of problems, the transient phenomenon of the heat conduction in the thick-film structure can be neglected because of the "thermal inertia" of the whole system. Although such a limitation has an influence on the simulation results because higher temperatures can be obtained during the transient, the steady-state thermal conditions are considered in many cases. The steady temperature distribution in an object means that the heat leaving

any volume element equals the quantity produced. Since  $\partial T / \partial t = 0$  in the mathematical statement (1), the heat-transfer equation can be written as:

$$\nabla(-\lambda \cdot \nabla T) - q_v = 0 \quad (5)$$

Convection is the transfer of heat from bounding surfaces to a fluid, and defines the heat-exchange conditions at the boundary of the solid body. A mathematical formulation of the heat flow  $H_d$  dissipated across the surface  $A$  of the body into an environment of ambient temperature  $T_a$  is given by:

$$H_d = \alpha \cdot A \cdot (T - T_a) \quad (6)$$

Depending upon the cause of the fluid motion a distinction is made between free, or natural, convection and forced convection. In either case, the convection can be expressed using a heat-transfer coefficient  $\alpha$ , the quantity that characterises the intensity of the heat transfer and depends upon the method of cooling. The natural convection heat-transfer coefficient is usually obtained using empirically derived relationships, which have been found to work well in practice. For forced convection,  $\alpha$  can be estimated as  $\alpha = \sqrt{2v/L}$ , where  $v$  is the air velocity and  $L$  is the length of the body.

The thermal radiation is governed by the equation:

$$E_T = \sigma \cdot \varepsilon \cdot A (T^4 - T_a^4) \quad (7)$$

where  $E_T$  is the heat flow radiated through the surface  $A$ ,  $\sigma$  is the Stefan-Boltzman constant,  $T_a$  is the ambient temperature and  $\varepsilon$  is the surface emissivity.

In a finite-element model the mathematical formulations of the heat transferred from the structure's outer surfaces by convection and radiation are commonly used to specify heat-exchange boundary conditions. The mathematical notation is:

$$-\lambda \nabla T \cdot n = \alpha \cdot (T - T_a) + \sigma \cdot \varepsilon \cdot (T^4 - T_a^4) \quad (8)$$

where  $-\lambda \nabla T$  is the outward heat flux from the boundary and  $n$  denotes the outward surface normal unit.

## 2.3 Modelling simultaneous electric and thermal conduction

Generally, electronic circuits are heated by the power dissipated in the components. The heating caused by an electric current flowing through a thick-film resistor depends not only on the total power dissipated in the component but also on its geometry. In cases when non-conventional shapes of thick-film resistors are used the heating becomes non-uniform and both the conduction of charge and the conduction of heat should be considered simultaneously. A similar situation occurs in the cases when the resistor is

trimmed, because the trim cut causes a non-uniform distribution of the current density in the region of the resistor. In order to calculate both the potential and the temperature distribution for the steady-state conditions we combine equations (3) and (5). By taking  $q_v = J \times E = (-\gamma \nabla U) \cdot (-\nabla U)$  for the heating power source term, the following system of simultaneous equations needs to be resolved:

$$\begin{aligned} \nabla(-\gamma \nabla U) &= 0 \\ \nabla(-\lambda \nabla T) - \gamma (\nabla U)^2 &= 0 \end{aligned} \tag{9}$$

In general, both the thermal conductivity  $\lambda$  and the electrical conductivity  $\sigma$  depend on the temperature. By introducing the temperature dependency of the resistivity  $\rho = 1/\gamma$  in the form:  $\rho = \rho_0 \cdot \left(1 + a \cdot T + b \cdot T^2\right)$ , where  $\rho_0$  is the resistivity at 0°C and  $a$  and  $b$  are the temperature coefficients of the resistivity of the resistor layer, a variety of thick-film materials can be described. Negative thermistor thick-film materials exhibit response curves similar to the discrete NTC thermistors so that the temperature characteristics can be expressed with the well-known expression:

$$\rho_T = \rho_N \cdot e^{\beta \left(\frac{1}{T} - \frac{1}{T_N}\right)} \tag{10}$$

where  $\rho_T$  is the resistivity at temperature  $T$ ,  $\rho_N$  is the resistivity at temperature  $T_N$ .  $T$  and  $T_N$  are temperatures in Kelvin and  $\beta$  is a material-specific parameter.

### 3. FEA-driven designs of the thick-film structures

#### 3.1 Analysis of a thick-film resistor

The thick-film resistor is an elementary component of a thick-film circuit. It is made by screen-printing the thick-film resistor material and the metallic end-contact material, which provide electrical connections onto a ceramic substrate. Figure (1) shows the design of a typical thick-film resistor.

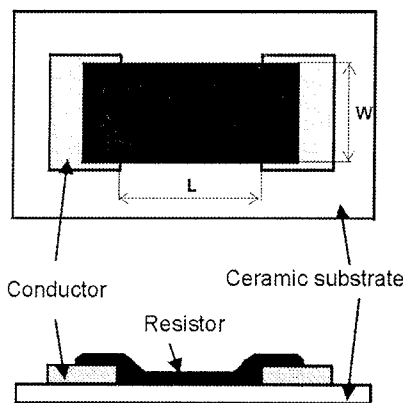


Figure 1. Typical geometry of a thick-film resistor, the top-view and the cross-section

The actual value of the resistance is determined from the resistivity of the resistor material at the recommended deposition thickness, which is usually quoted in ohms per square (sheet resistivity) and the designed aspect ratio  $L/W$ . The relation is given by the following equation:

$$R = \rho \cdot \frac{L}{W \cdot t} = R_{sh} \cdot \frac{L}{W} \tag{11}$$

where  $\rho$  is the resistivity of the material,  $L$  is the resistor length,  $W$  is the resistor width,  $t$  is the thickness and  $R_{sh}$  is the sheet resistivity. Commercially available thick-film resistor materials have sheet resistivities in decade values from 1Ω per square to 10 MΩ per square for typical layer thicknesses, which are in the range 5μm to 20μm. From relation (11) we can see that designers have a degree of flexibility when laying out a particular circuit design. In practice, deviations from the designed values are regularly adjusted by laser trimming. This changes the resistor geometry and introduces new critical points in the resistor design. In some applications the influence of the trimming cut on the resistors' performance should be analysed. This becomes more important with high-power applications, where the shape of the laser cut influences the temperature distribution in the resistor; and in sensor applications, where the resistance of the thick-film resistors depends on the resistor position and any local strains. Figure 2 presents the simulated current density for thick-film resistors of a typical shape, which exhibit bending of the current caused by a laser cut in the bottom resistor.

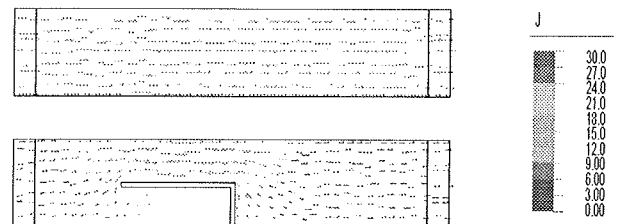


Figure 2. A 2D presentation of the current-density vector showing the bending of the current flow lines caused by a laser cut

The changes to the current density caused by the laser cut affect the temperature distribution in the resistor. For this reason the design of power hybrids often requires an analysis of the laser-cut shape on the power resistor. The self-heating effect of the thick-film resistor can be modelled using the system of equations (9). Figure 3 shows the steady-state temperature distribution in the trimmed resistor from Figure 2 in the case where a voltage of 50V was applied to its ends and the natural air convection ( $a = 10$ ) on the outer boundaries was modelled by (8). Normally, the maximum temperature is expected in the middle of the resistor. Depending on the laser-cut position, the hottest point in the resistor can be moved towards the regions of higher current density.

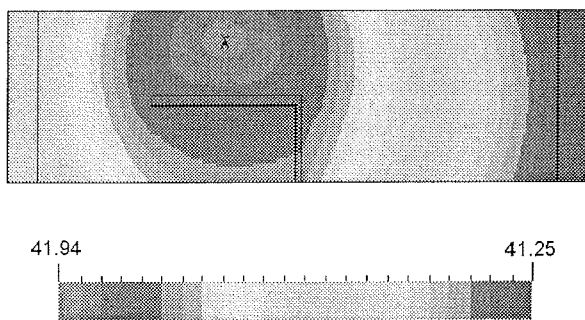


Figure 3. Temperature distribution in the self-heated thick-film resistor

Sometimes, depending on the application, an unconventional thick-film resistor geometry (shape) is designed. In such cases the relation (11) is no longer valid. Generally, the resistance is a global quantity depending on the solution of a simple boundary-value problem using Laplace's equation (3). For more complicated boundaries exact solutions are not available and some special non-trivial mathematical approaches [8] have to be used. In any event, the solution can be evaluated numerically using the finite-element approach. In this way the resistance of a thick-film resistor can be computed by evaluating the current through the resistor, as a surface integral of the normal component of the current density  $J$  over the surface of the cross-section of the resistor. The relation  $R = \Delta U/I$ , where  $\Delta U$  is the potential difference at its end-contact boundaries, can then be used. For example, the numerically obtained resistance of the untrimmed resistor from Figure 2, for  $R_{sh} = 100 \Omega/\text{square}$ , is  $450 \Omega$  and the resistance of the trimmed resistor is  $628 \Omega$ . In this simple case the resistance of the untrimmed resistor can be verified using formula (11).

An example of an analysis of an unconventional thick-film resistor is presented in Figure 4. The figure shows the current-density distribution in the specially shaped 'delta' resistor, which was designed for a ceramic pressure-sensor application. The resistor regions where the current density is higher exert more of an influence on the total resistance. The calculated value of the resistance is  $2.375 \cdot R_{sh}$ .

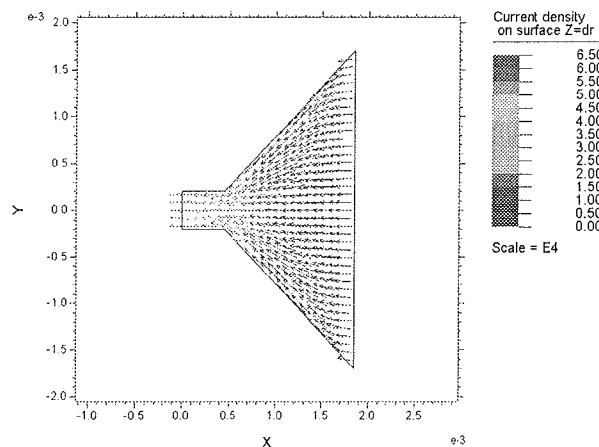


Figure 4. The current density in an unconventional thick-film resistor

### 3.2 Optimisation of a hybrid power-module design

In order to provide reliable operation of hybrid thick-film power modules it is important to maintain the operating temperature of each component and the whole circuit, within the allowed limits. Although the power circuits are usually mounted on appropriate heat sinks to enable effective cooling, extra precautions have to be taken when designing the circuit layout. In such cases a simulation of the electro-thermal behaviour has proved useful. In the following we describe how a finite-element analysis was used in the design-optimisation phase of a hybrid power module that is part of an electricity meter. The main purpose of the simulations was to help the designer to redraw the circuit layout by reducing the thick-film resistor area in such a way that its resistance and maximum allowed temperature of the substrate remain unchanged. This allowed for a reduction of the module prime costs.

The treated hybrid thick-film circuit is installed in a plastic (crastine) housing as shown in Figure 5. Figure 6 shows a schematic representation of the module's cross-section.

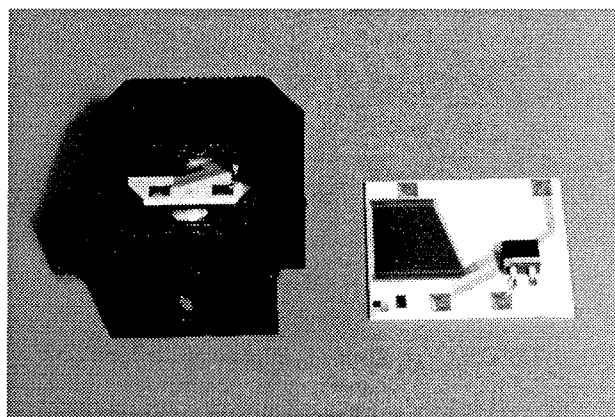
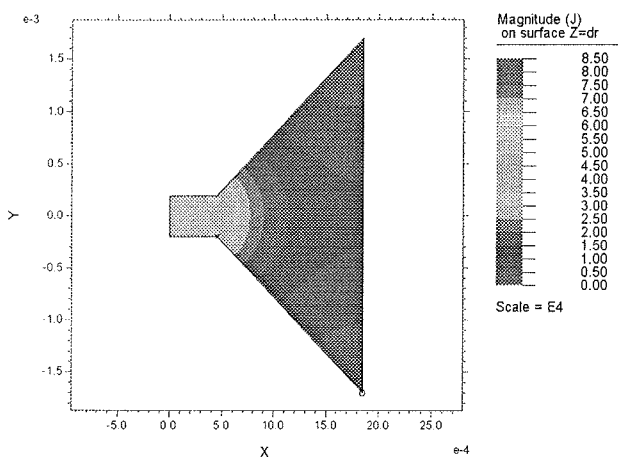


Figure 5. View of the treated power-hybrid thick-film circuit installed in the crastine housing

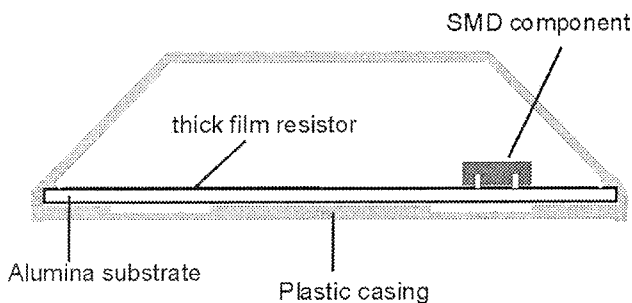


Figure 6. Schematic representation of the module's cross-section

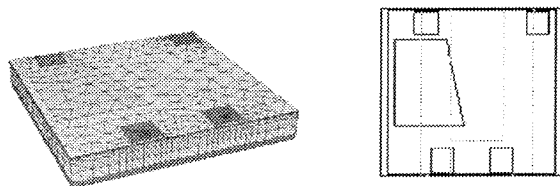


Figure 7. Simplified 3D geometry of the structure and its projection onto the X-Y plane

The whole construction was mounted on the rear of the electricity-meter housing, which was at ambient temperature. The circuit was heated by an electric current flowing through the thick-film resistor. The heat rise as a result of the SMD component power dissipation had a relatively small influence

on the temperature profile of the whole module and was not included in the model. Since there was no additional heat sink the circuit was only cooled through the metal connections to the main part of the device and only natural air convection had to be treated on the structure boundaries. The plastic housing was uncovered on two sides allowing the influence of its upper part to be neglected. The simplified structure geometry is presented in Figure 7. Steady-state thermal conditions in the structure were modelled with equation (5), and the heat-transfer boundary conditions formulated using (6). Although simplifications to the circuit geometry and boundary conditions were made, the achieved accuracy of the model was less than 5%. A detailed description of the finite-element model and its experimental verification is presented in /9/.

In order to meet the required electrical and thermal performance, various circuit layouts were considered. Our simulations indicated that a reduction in the size of the thick-film resistor by 50% would increase the maximum temperature of the whole circuit by 10%. However, by shifting the resistor nearer to the metal pads a lower value for the maximum temperature was achieved. A simulated temperature distribution on the top of the substrate for different layout options is presented in Figure 8.

Simulations of the optimised circuit layout showed that a maximum temperature below 68°C could be achieved. Realisation in practice confirmed the validity of the simulated results.

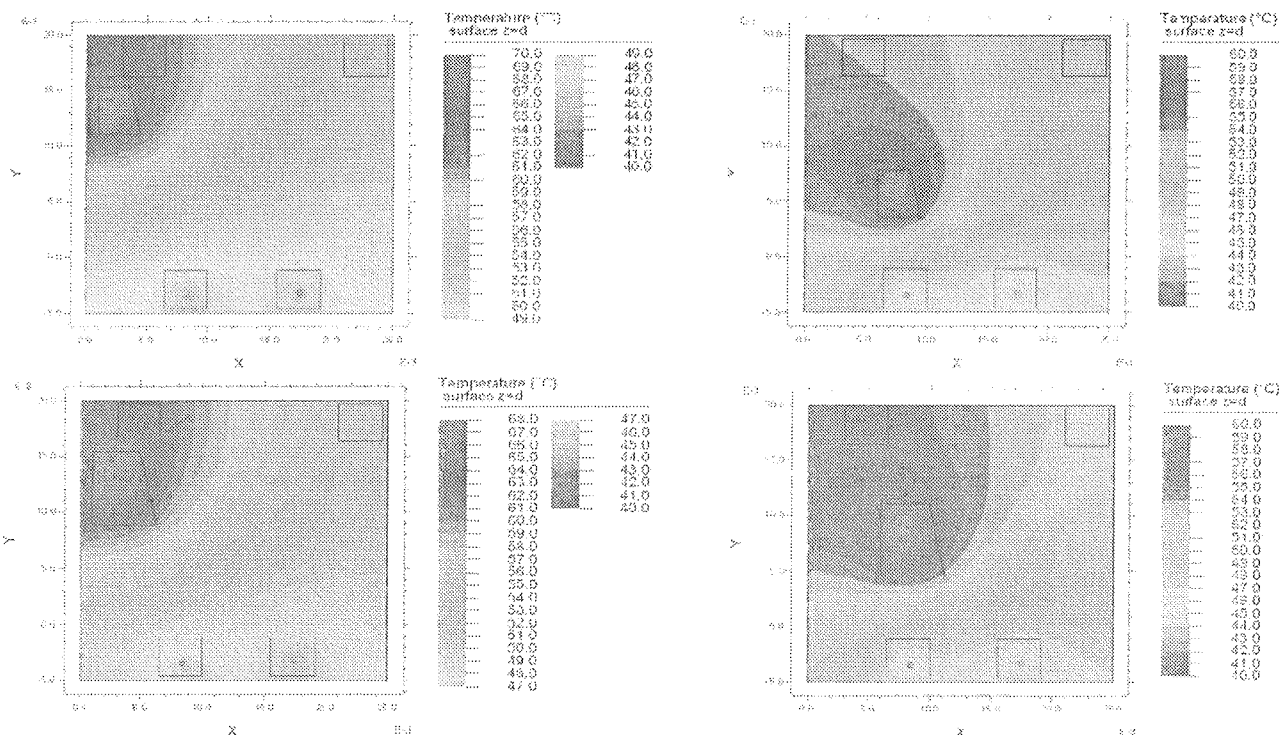


Figure 8. Steady-state temperature distribution on the surface of the thick-film substrate for four different layouts (ambient temperature  $T_{amb} = 40^{\circ}C$ )

### 3.3. Transient electro-thermal analysis of an over-current-protection module

An over-current-protection thick-film hybrid module containing SMD PTC thermistors as self-resetting overload-protection elements was designed for protecting a communication line against a surge current resulting from lightning or accidental shorts between adjacent power feed lines. Figure 9 shows the over-current-protection module for the symmetric protection of telecommunication systems containing two symmetric circuits for protection. Each circuit includes thick-film resistors in series with a PTC thermistor between the input node, which is coupled to the communication line, and the output node, which is linked to the target equipment being protected. When the over-current enters such a protection module the thermistors self-heat and rapidly increase their resistance, providing protection for the associ-

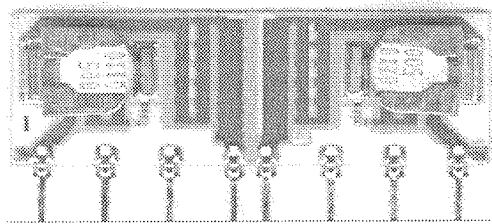


Figure 9. The over-current-protection module for the symmetric protection of telecommunication systems containing two symmetric circuits for protection

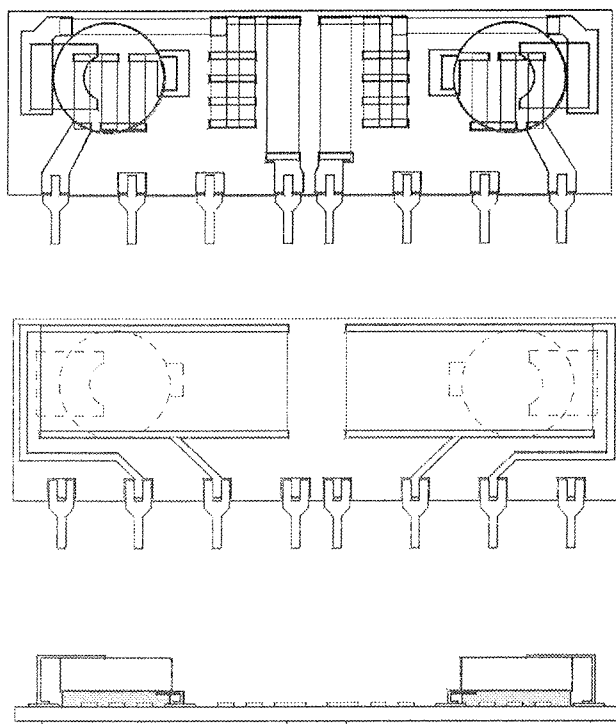


Figure 10. The front and rear layouts and the cross-section of the over-current-protection circuit

ated equipment by suppressing the surge current. In the presented circuit the thermistors are also heated externally by the heat dissipating from the thick-film resistors, which are connected through the external circuit connections and located on the rear of the substrate. The schematic representations of the circuit's front and rear layouts, and the cross-section are given in Figure 10.

The location of the heat sources and their sizes as well as the thermal properties of the substrate and other materials used, play a fundamental role in determining the temperature distribution in a hybrid thick-film circuit and thereby affect the circuit's response characteristics. A transient finite-element thermal analysis was performed to predict the dynamic temperature states at the critical points of the circuit design and to find the hybrid circuit arrangement that provides the most reliable circuit operation.

In order to keep the model size manageable, while maintaining sufficient element density in the regions of interest, some assumptions and simplifications relating to the circuit geometry were performed. The resistors dissipating a negligible amount of heat in comparison with the heat dissipated in the thick-film resistor on the rear were excluded from the model. The influence of the thick-film resistor overglaze on the temperature distribution within the whole module is estimated to be quite small and therefore omitted. The fraction of the heat transferred by conduction through the connection wires during the transient (for  $t < 15$  sec) has a small influence on the temperature distribution in the region of the PTC thermistor and the thick-film resistor on the rear of the substrate and it can be neglected. Applying half-symmetry boundary conditions for the heat exchange between the two symmetrical parts of the module additionally reduced the model size. The simplified 3D geometry of the model is presented in Figure 11.

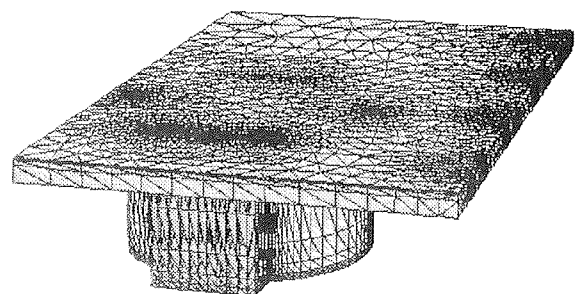


Figure 11. View of the meshed 3D model of the module

The transient thermal situation was modelled using the heat-transfer equation (4), where the internal heating term  $q_v$  represents the heat per unit volume generated in the regions of the resistive elements. Therefore,  $q_v$  can be determined as the mean power dissipated in the PTC thermistor and the thick-film resistor regions. It can be calculated in the same way as in the previous example, e.g. by calculating the potential distribution and the current density in the circuit structure and by solving the system of equations (5). In order to

reduce the number of required numerical calculations and to shorten the simulation time the term  $q_v$  was defined by a piecewise linear approximation of the power dissipated in the regions of the thick-film resistor and the hermistor as function of the instantaneous temperature of the thermistor. The heat-exchange boundary conditions on the circuit's outer surfaces were specified by (8).

The objective of the analysis was to track the temperature distribution in the PTC thermistor and the thick-film resistor on the rear of the ceramic substrate during the period in which the over-current flows through the circuit. Figure 12 shows the temperature distribution in the cross-section of the module after 10 sec.

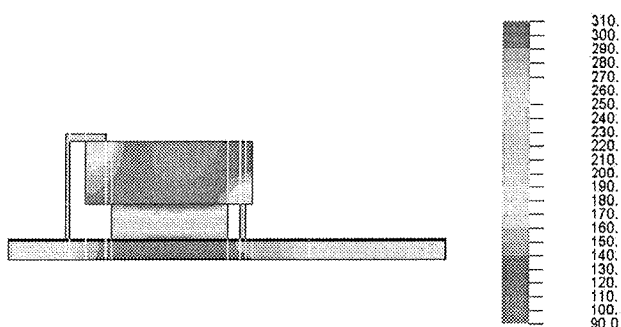


Figure 12. Temperature distribution in the cross-section of the structure after 10 sec

Because the temperature distribution within the body of the thermistor depends on the distance from the component's metal connections the temperature in the geometric middle of the component was regarded as the actual instantaneous temperature of the whole thermistor element. Based on this assumption it is evident from Figure 12 that the instantaneous temperature of the thermistor element reaches its specified reference temperature of 120°C after 10 sec. This result corresponded to the measured switching time of the module /10/, which confirmed the correctness of the model. At the same time the temperature on the surface of the thick-film resistor increased to its maximum value of 330°C. The temperature distribution on the rear of the module after 10 sec is presented in Figure 13. After the thermistor has

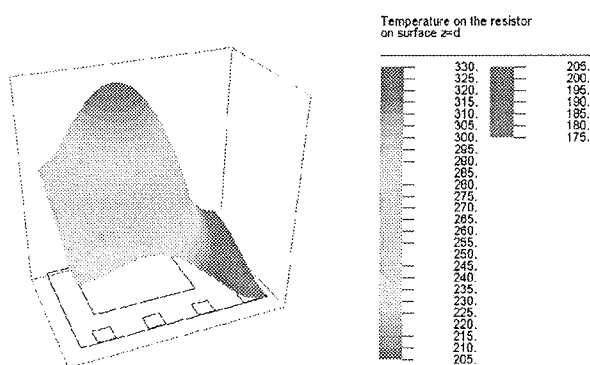


Figure 13. Temperature distribution on the rear of the substrate after 10 sec

limited the current flow through the circuit the temperature of the resistor on the rear starts to fall. Simultaneously, the effect of the cooling through the connection pads becomes more evident. The temperature situation on the rear side after 20 sec is presented in Figure 14.

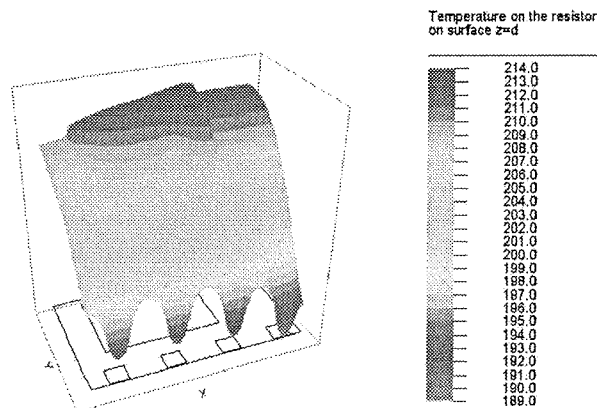


Figure 14. Temperature distribution on the rear of the substrate after 20 sec

The described model was used to explore the changes in the switching time depending on the thick-film resistor area and the amount of adhesive used for bonding the thermistor to the substrate. Minimising the thick-film-resistor area lead to higher local temperatures in the circuit, which may influence the component to change its resistance or even burn up the resistor. To avoid such undesirable situations different design options were analysed. The simulations helped us find the optimum resistor dimensions and position. Additionally, a FEA was performed for the case study concerning situations in which the adhesive covers different expanses of the thermistors' surface. Simulations showed that the amount of adhesive significantly influenced the maximum temperature and the switching time of the module. Simulated temperature distributions in the thermistor and the thick-film resistor for the cases when 50%, 70%, and 100% of the thermistors' surface was covered by adhesive are presented in Figures 15 and 16.

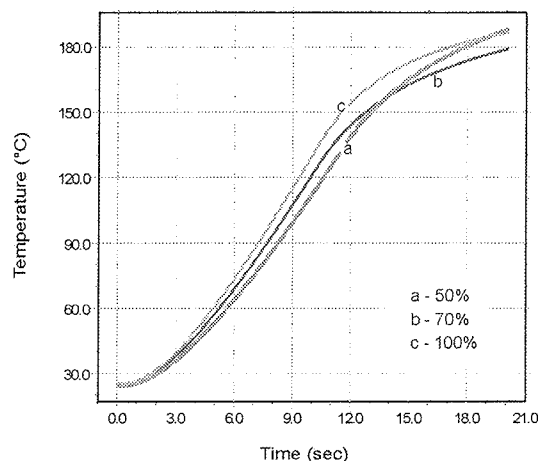


Figure 15. Dynamic temperature states in the geometric middle of the PTC thermistor

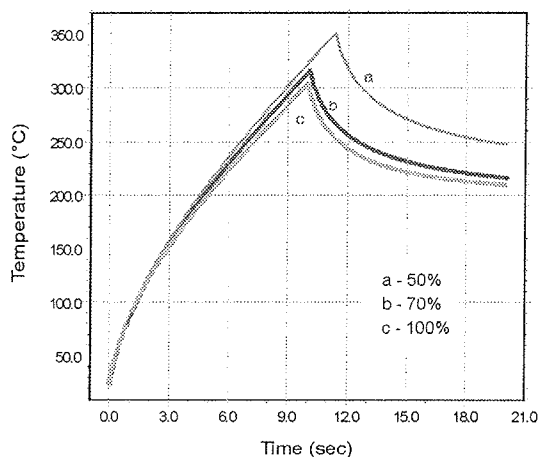


Figure 16. Dynamic temperature states in the thick-film resistor on the rear of the circuit

Figure 15 shows the temperature tracks in the middle of the PTC thermistor during a period of 20 sec. A temperature of 120°C, which corresponds to the thermistor reference temperature, determines the switching time of the module. It is evident from the curves in Figure 15 that the changes in the switching time are less than 3 sec. The temperature tracks presented in Figure 16 indicate that a lower maximum temperature in the thick-film resistor can be achieved for a more extensive coverage of the thermistor area by the adhesive. Simulations showed that at least 70% of the thermistor surface has to be covered to keep the maximum temperature in the acceptable range.

The temperature on the surface of the thermistor and the thick-film resistor was measured with an infrared temperature probe. Such a low-cost method for measuring temperature was based on our experience of earlier, similar applications /11/, and proved to be satisfactory in practice. Furthermore, probe measurements at different locations in combination with software tools for temperature monitoring (like, for example /12/) can be used for the verification of the numerical model.

#### 4. Summary

This paper describes our experience of applying finite-element analyses in the design of thick-film hybrids. Three different case studies that give some insight into the electrical and thermal situations in the thick-film structure were discussed. Simulations were performed to analyse the electrical and thermal behaviour of unconventionally shaped thick-film resistors and to calculate their resistances. FEA of the electro-thermal properties of a thick-film hybrid power module was performed and the optimum circuit layout was determined. Furthermore, a transient electro-thermal analysis was used for the design optimisation of an over-current-protection circuit. We can conclude that a finite-element code can be successfully introduced to the design cycles to reveal critical points in the design and help to find the optimum design solution.

#### Acknowledgement

I wish to thank HIPOT-HYB for providing samples of the hybrid circuits and for permission to publish some design details. The technical assistance given by Srečko Maček (Jožef Stefan Institute, Ljubljana) is gratefully acknowledged. The work was financially support by the Ministry of Education, Science and Sport of the Republic of Slovenia (Grant No L2-2447).

#### REFERENCES

- /1/ A.Langari, H.Hashemi, „Transient Thermal Analysis of a Power Amplifier Module”, Proceedings of International Symposium on Microelectronics, 1998, pp.844-849.
- /2/ L.A. Barcia, S.O.Velasco, C.Q.Guia, „Finite Element Analysis in the Design of a Power Converter”, 9th.European Hybrid Microelectronics Conference, Nice 1993, pp.421-430.
- /3/ Johannes Adam, “Don't waste time: simulate!”, Proceedings of European Microelectronics and Packaging Conference 2001, pp. 844-849.
- /4/ Jaroslav Kita, Andrzej Dziedzic, Kazimierz Fredel, LeszekJ. Golonka, Pawel Janus, Roman Szeloch, “Temperature Distribution Analysis in Sensors with Buried Heater Made in LTCC Technology”, Proceedings of European Microelectronics and Packaging Conference 2001, pp. 123-128.
- /5/ T.Zawada, A. Dziedzic, L.J.Golonka, G.Hanreich, J.Nicolics, “Temperature field analysis in a low temperature cofired ceramic microsystem”, Proc. IMAPS-Europe 2000, pp. 388-393.
- /6/ Mark J. Vesilgaj, Cristina H. Amon, “Transient Thermal Management of Temperature Fluctuations During Time Varying Workloads on Portable Electronics”, IEEE Transaction on Computers and Packaging Technology, Vol. 22, No 4, 1999.
- /7/ Ryszard J. Pripitniewicz, Steven A. Weller, Sam R.Shaw, William L.Herb, “Computational modeling and simulation of thermal effects in a new design of a small form-factor pluggable (SFP) system”, Proc. International symposium on Microelectronics, Boston, 2000, pp. 381-386.
- /8/ L. N. Trefethen, “Analysis and design of polygonal resistors by conformal mapping”, Journal of applied mathematics and physics, Vol. 35, September 1984.
- /9/ M. Santo Zarnik, S. Maček, “Thermal modelling and optimisation of hybrid thick-film structures”, Proceedings of International Conference IMAPS-Poland, 2000, pp. 269-275.
- /10/ M. Santo Zarnik, S. Maček, “A finite element analysis of the electro-thermal characteristics of an over-current-protection thick-film hybrid module”, Proceedings of International Conference MIDEM 2001, pp. 273-278.
- /11/ M. Santo Zarnik M., Novak F, Macek S, Design for test of crystal oscillators: A case study. *Journal of electronic testing: Theory and Applications* 1997 11: 109-117.
- /12/ Marko Lamot, Borut Žalik, “Software tool for the support of on-line thermal monitoring of microelectronic systems”, Informacije MIDEM, Vol 30, No. 3, 2000, pp 144-147.
- /13/ Gunnar Backstrom, “Fields of Physics by Finite Element Analysis, An Introduction”, Studentlitteratur, Lund 1998.

Marina Santo Zarnik  
HIPOT - RR, d.o.o., c/o Institut “Jožef Stefan”  
Jamova 39, 1000 Ljubljana, Slovenia,  
Tel: +386 1 4773 583, Fax: +386 1 4263 126  
e-mail: marina.santo@ijs.si